The tryptophan salvage pathway is dynamically regulated by the iron-dependent repressor YtgR in *Chlamydia trachomatis*

Nick D. Pokorzynski[1] and Rey A. Carabeo[1]

[1]Center for Reproductive Biology, School of Molecular Biosciences, College of Veterinary Medicine, Washington State University, Pullman, WA, USA, 99164.

Corresponding Author:

Rey A. Carabeo

1770 NE Stadium Way, Biotechnology & Life Sciences Bldg., Washington State University

Pullman, WA, 99164

(509) 335-7788

rey.carabeo@wsu.edu

Keywords: stress response, transcription, tryptophan biosynthesis, iron-dependent regulation, repression

Abstract

Mammalian hosts restrict cellular nutrient availability to starve invading pathogens and successfully clear an infection by a process termed “nutritional immunity”. For the obligate intracellular pathogen *Chlamydia trachomatis*, nutritional immunity likely encompasses the simultaneous limitation of the amino acid tryptophan and the essential biometal iron. Unlike other model bacteria, *C. trachomatis* lacks many global stress response systems – such as “stringent response” homologs – adapted to these host insults. However, a physiological response by *Chlamydia* that is common to both stresses is the development of an aberrant, “persistent” state, suggesting that tryptophan and iron starvation trigger a coordinated developmental program. Here, we report that the *trpRBA* operon for tryptophan salvage in *C. trachomatis* serovar L2 is regulated at the transcriptional level by iron. The expression of the tryptophan synthase encoding genes, *trpBA*, is induced following iron limitation while that of the repressor *trpR* is not. We show that this specific induction of *trpBA* expression initiates from a novel promoter element within an intergenic region flanked by *trpR* and *trpB*. YtgR, a DtxR-homolog and the only known iron-dependent transcriptional regulator in *Chlamydia*, can bind to the *trpRBA* intergenic region upstream of the alternative *trpBA* promoter to repress transcription. This binding also likely attenuates transcription from the primary promoter upstream of *trpR* by blocking RNA polymerase read-through. These data illustrate a dynamic and integrated method of regulating tryptophan biosynthesis in an iron-dependent manner, which has not been described in any other prokaryote, underscoring the uniqueness of *Chlamydia*.

Significance Statement

Genital serovars of the obligate intracellular parasite *Chlamydia trachomatis* are the leading cause of bacterial sexually-transmitted infections globally. Proliferation of *C. trachomatis* is likely controlled by simultaneous immunological and environmental restriction of critical nutrients such as tryptophan and iron. However, our understanding of the immediate chlamydial responses to these stimuli is poorly defined. We utilized expression of the stress-responsive *trpRBA* operon in *C. trachomatis* L2 as a proxy for regulatory integration between iron and tryptophan limitation. We identified a unique iron-dependent regulatory mechanism for *trpRBA* in *C. trachomatis*, mediated by the transcriptional repressor YtgR. This distinguishes *Chlamydia* from other bacteria which regulate tryptophan biosynthesis strictly by tryptophan-dependent mechanisms, highlighting a distinct evolutionary adaptation in *C. trachomatis* to integrate stress responses.

/body

Introduction

Nutrient acquisition is critical for the success of pathogenic bacteria. Many pathogenic bacteria must siphon nutrients from their hosts, such as nucleotides, amino acids and biometals (1–4). This common feature among pathogens renders them susceptible to nutrient limitation strategies associated with the host immune response (5). Counteractively, bacterial pathogens have evolved sophisticated molecular mechanisms to counter nutrient deprivation, involving increasingly complex and sophisticated nutrient-sensing regulatory networks. These stress response mechanisms are essential for pathogens to avoid clearance by the immune system. By delineating their function at the molecular level, we can better target aspects of the host-pathogen interface suitable for therapeutic manipulation. However, stress responses in the obligate intracellular bacterium *Chlamydia trachomatis* are relatively poorly characterized, leaving unanswered many fundamental questions about the biology of this pathogen.

Chlamydia trachomatis is the leading cause of bacterial sexually transmitted infections (STIs) and infection-derived blindness worldwide (6–8). Genital infections of chlamydia are associated with serious sequelae in the female reproductive tract such as tubal factor infertility (9). Chlamydiae are Gram-negative bacterial parasites that develop within a pathogen-specified membrane-bound organelle termed the inclusion (10). Chlamydial development is uniquely characterized by a biphasic interconversion of an infectious elementary body (EB) with a non-infectious, but replicative reticulate body (RB) (11). An obligate intracellular lifestyle has led to reductive genome evolution

93 across chlamydial species; Chlamydiae have retained genes uniquely required for their
94 survival, but have become nutritionally dependent on their hosts by discarding many
95 metabolism-related genes (12). Of note, *C. trachomatis* does not possess genes
96 necessary for eliciting a stringent response to nutrient starvation (*e.g. relA, spoT*),
97 suggesting that this pathogen may utilize novel mechanisms to respond to stress (13).
98 It is well established, however, that in response to various stressors, Chlamydiae
99 deviate from their normal developmental program to initiate an aberrant developmental
100 state, termed “persistence” (14). This persistent state is distinguished by the presence
101 of viable, but non-cultivable, abnormally enlarged chlamydial organisms that display
102 dysregulated gene expression. Importantly, *Chlamydia* can be reactivated from
103 persistence by abatement of the stress condition. As such, chlamydial persistence at
104 least superficially resembles a global stress response mechanism. Yet the molecular
105 underpinnings of this phenotype are poorly understood, with most published studies
106 focusing on the molecular and metabolic character of the aberrant, persistent form. It is
107 therefore unclear to what extent primary stress responses contribute to the global
108 persistent phenotype in *Chlamydia*.
109 The best described inducer of persistence is the pro-inflammatory cytokine
110 interferon-gamma (IFN-γ). The bacteriostatic effect of IFN-γ has been primarily
111 attributed to host cell tryptophan (Trp) catabolism, for which *C. trachomatis* is
112 auxotrophic (15–17). Following IFN-γ stimulation, infected host cells up-regulate
113 expression of indoleamine-2,3-dioxygenase (IDO1), which catabolizes Trp to *N*-
114 formylkynurenine via cleavage of the indole ring (18). *C. trachomatis* cannot recycle
115 kynurenines, unlike some other chlamydial species (19), and thus IFN-γ stimulation

116 effectively results in Trp starvation to *C. trachomatis*. The primary response to Trp
117 starvation in *C. trachomatis* is mediated by a TrpR ortholog, whose Trp-dependent
118 binding to cognate promoter elements represses transcription (20, 21). This
119 mechanism of regulatory control is presumably limited in *C. trachomatis*, as homologs of
120 genes regulated by TrpR in other bacteria (*e.g. trpF, aroH, aroL*) have not been shown
121 to respond to Trp limitation (22).

122 In many Gram-negative bacteria, such as *Escherichia coli*, *trpR* is monocistronic
123 and distal to the Trp biosynthetic operon. In *C. trachomatis,* TrpR is encoded in an
124 operon, *trpRBA*, which also contains the Trp synthase α- and β- subunits (TrpA and
125 TrpB, respectively), and possesses a 351 base-pair (bp) intergenic region (IGR) that
126 separates *trpR* from *trpBA*. The functional significance of the *trpRBA* IGR is poorly
127 characterized; while a putative operator sequence was identified overlapping an
128 alternative transcriptional origin for *trpBA* (20), the IGR was not shown to be bound by
129 TrpR (21). Based on *in silico* predictions, an attenuator sequence has been annotated
130 within the *trpRBA* IGR (23), but this has not been thoroughly validated experimentally.
131 Regardless, the IGR is more than 99% conserved at the nucleotide sequence level
132 across ocular, genital and lymphogranuloma venereum (LGV) serovars of *C.*
133 *trachomatis*, indicating functional importance (Fig. S1). Therefore, relative to other
134 model bacteria, the regulation of the *trpRBA* operon remains poorly elucidated.

135 In evaluating alternative regulatory modes of the *trpRBA* operon, an interesting
136 consideration is the pleiotropic effects induced by IFN-γ stimulation of infected cells.
137 IFN-γ is involved in many processes that limit iron and other essential biometals to
138 intracellular pathogens as a component of host nutritional immunity (5, 24). *Chlamydia*

have a strict iron dependence for normal development, evidenced by the onset of persistence following prolonged iron limitation (25). Importantly, *Chlamydia* presumably acquire iron via vesicular interactions between the chlamydial inclusion and slow-recycling transferrin (Tf)-containing endosomes (26). IFN-γ is known to down-regulate transferrin receptor (TfR) expression in both monocytes and epithelial cells with replicative consequences for resident intracellular bacteria (27–30). However, iron homeostasis in *Chlamydia* is poorly understood, due to the lack of functionally characterized homologs to iron acquisition machinery that are highly conserved in other bacteria (31). Only one operon, represented by *ytgABCD*, has been clearly linked to iron acquisition. The periplasmic metal-binding protein YtgA displays a specific binding affinity for ferric iron over other divalent cations and likely transports iron from the outer membrane to an ABC-3 type inner membrane metal permease formed by the YtgBCD complex (32). Intriguingly, the YtgC (CTL0323) open reading frame (ORF) encodes a N-terminal permease domain fused to a C-terminal DtxR-like repressor domain, annotated YtgR (33, 34). YtgR is cleaved from the permease domain during infection and functions as an iron-dependent transcriptional repressor to autoregulate the expression of its own operon (34). YtgR represents the only identified iron-dependent transcriptional regulator in *Chlamydia.* Whether YtgR maintains a more diverse transcriptional regulon beyond the *ytgABCD* operon has not yet been addressed and remains an intriguing question in the context of immune-mediated iron limitation to *C. trachomatis*. Crucially, simultaneous IFN-γ-mediated iron and Trp starvation raise the possibility that *C. trachomatis* could have evolved an integrated response to multiple stresses.

Consistent with the highly reduced capacity of the chlamydial genome, it is likely that *C. trachomatis* has a limited ability to tailor a specific response to each individual stress. In the absence of identifiable homologs for most global stress response regulators in *C. trachomatis*, we hypothesized that primary stress responses to pleiotropic insults may involve mechanisms of regulatory integration, whereby important molecular pathways are co-regulated by stress-responsive transcription factors such that they can be utilized across multiple stress conditions simultaneously induced by the host. Here, we report on the unique iron-dependent regulation of the *trpRBA* operon in *Chlamydia trachomatis.* We propose a model of iron-dependent transcriptional regulation of *trpRBA* mediated by the repressor YtgR binding specifically to the IGR, which may have implications for how *C. trachomatis* responds to immunological and environmental insults. Such a mechanism of iron-dependent regulation of Trp biosynthesis has not been previously described in any other prokaryote and adds to the catalog of regulatory models for Trp biosynthetic operons in bacteria. Further, it reveals a highly dynamic mode of regulatory integration within the *trpRBA* operon, exemplifying the importance of this pathway to chlamydial stress response.

Results

Brief iron limitation via 2,2-bipyridyl treatment yields iron-starved, but non-persistent *Chlamydia trachomatis.* To identify possible instances of regulatory integration between iron and Trp starvation in *C. trachomatis*, we optimized a stress response condition that preceded the development of a characteristically persistent phenotype. We reasoned that in order to effectively identify regulatory integration, we would need to investigate the bacterium under stressed, but not aberrant, growth

conditions such that we could distinguish primary stress responses from abnormal growth. To specifically investigate the possible contribution of iron limitation to a broader immunological (*e.g.* IFN-γ-mediated) stress, we utilized the membrane-permeable iron chelator 2,2-bipyridyl (Bpdl), which has the advantage of rapidly and homogeneously starving *C. trachomatis* of iron (35). We chose to starve *C. trachomatis* serovar L2 of iron starting at 12 hrs post-infection (hpi), or roughly at the beginning of mid-cycle growth. At this point the chlamydial organisms represent a uniform population of replicative RBs that are fully competent, both transcriptionally and translationally, to respond to stress. We treated infected HeLa cell cultures with 100 μM Bpdl or mock for either 6 or 12 hours (hrs) to determine a condition sufficient to limit iron to *C. trachomatis* without inducing hallmark persistent phenotypes. We stained infected cells seeded on glass coverslips with convalescent human sera and analyzed chlamydial inclusion morphology under both Bpdl- and mock-treated conditions by laser point-scanning confocal microscopy (Fig. 1A). Following 6 hrs of Bpdl treatment, chlamydial inclusions were largely indistinguishable from mock-treated inclusions, containing a homogeneous population of larger organisms, consistent with RBs in mid-cycle growth. However, by 12 hrs of Bpdl treatment, the inclusions began to display signs of aberrant growth: they were perceptibly smaller, more comparable in size to 18 hpi, and contained noticeably fewer organisms, perhaps indicating a delay in RB-to-EB differentiation. These observations were consistent with our subsequent analysis of genome replication by quantitative PCR (qPCR; Fig. 1B.) At 6 hrs of Bpdl treatment, there was no statistically distinguishable difference in genome copy number when compared to the equivalent mock-treated time-point. However, by 12 hrs of treatment, genome copy

number was significantly reduced 4.7-fold in the Bpdl-treated group relative to mock-treatment (p = 0.0033). We then assayed the transcript expression of two markers for persistence by reverse transcription quantitative PCR (RT-qPCR): the early gene *euo*, encoding a transcriptional repressor of late-cycle genes (Fig.1C), and the adhesin *omcB,* which is expressed late in the developmental cycle (Fig. 1D). Characteristic persistence would feature sustained high *euo* expression late into infection, and suppressed *omcB* expression throughout development. We observed that at 6 hrs of Bpdl treatment, there was no statistically distinguishable difference in either *euo* or *omcB* expression when compared to the mock-treatment. Still at 12 hrs of Bpdl treatment, *euo* expression was unchanged. However, *omcB* expression was significantly induced following 12 hrs of Bpdl-treatment (p = 0.00015). This was unexpected, but we note that *omcB* expression has been shown to vary between chlamydial serovars and species when starved for iron (31). Collectively, these data indicated that 6 hrs of Bpdl treatment was a more suitable time-point at which to monitor iron-limited stress responses.

We additionally assayed these same metrics following 6 or 12 hrs of Trp starvation by culturing cells in either Trp-replete or Trp-deplete DMEM-F12 media supplemented with fetal bovine serum (FBS) pre-dialyzed to remove amino acids. We observed no discernable change in inclusion morphology out to 12 hrs of Trp starvation (Fig. S2A), but genome copy numbers were significantly reduced 2.7-fold at this time-point (p = 0.00612; Fig. S2B). The transcript expression of *euo* (Fig. S2C) and *omcB* (Fig. S2D) did not significantly change at either treatment duration, but Trp-depletion did result in a 2.0-fold reduction in *omcB* expression, consistent with a more characteristic

persistent phenotype. These data therefore also indicated that 6 hrs of treatment would be ideal to monitor non-persistent responses to Trp limitation.

We next sought to determine whether our brief 6-hr Bpdl treatment was sufficient to elicit a transcriptional iron starvation phenotype. We chose to analyze the expression of three previously identified iron-regulated transcripts, *ytgA* (Fig. 2A), *ahpC* (Fig. 2B) and *devB* (Fig. 2C), by RT-qPCR under Bpdl- and mock-treated conditions (35, 36). In addition, we analyzed the expression of one non-iron-regulated transcript, *dnaB* (Fig. 2D), as a negative control (37). Following 6 hrs of Bpdl treatment, we observed that the transcript expression of the periplasmic iron-binding protein *ytgA* was significantly elevated 1.75-fold relative to the equivalent mock-treated time-point ($p = 0.0052$). However, we did not observe induction of *ytgA* transcript expression relative to the 12 hpi time-point. We distinguish here between *elevated* and *induced* transcript expression, as chlamydial gene expression is highly developmentally regulated. Thus, it can be more informative to monitor longitudinal expression of genes, *i.e.* their induction, as opposed to elevation relative to an equivalent control time-point, which may simply represent a stall in development. While we did not observe induction of *ytgA*, which would be more consistent with an iron-starved phenotype, we reason that this is a consequence of the brief treatment period, and that longer iron starvation would produce a more robust induction of iron-regulated transcripts. Note that the identification of *ytgA* as iron-regulated has only been previously observed following extended periods of iron chelation (32, 35, 38). Similarly, we observed that the transcript expression of the thioredoxin *ahpC* was significantly elevated 2.15-fold relative to the equivalent mock-treated time-point ($p = 0.038$) but was not induced relative to the 12 hpi time-point. The

transcript expression of *devB*, encoding a 6-phosphogluconolactonase involved in the pentose phosphate pathway, was not observed to significantly respond to our brief iron limitation condition, suggesting that it is not a component of the primary iron starvation stress response in *C. trachomatis.* As expected, the transcript expression of *dnaB*, a replicative DNA helicase, was not altered by our iron starvation condition, consistent with its presumably iron-independent regulation (37). Overall, these data confirmed that our 6-hr Bpdl treatment condition was suitable to produce a mild iron starvation phenotype at the transcriptional level, thus facilitating our investigation of iron-dependent regulatory integration.

Transcript expression of the *trpRBA* operon is differentially regulated by iron in *Chlamydia trachomatis.* Upon identifying an iron limitation condition that produced a relevant transcriptional phenotype while avoiding the onset of persistent development, we aimed to investigate whether the immediate response to iron starvation in *C. trachomatis* would result in the consistent induction of pathways unrelated to iron utilization/acquisition, but nevertheless important for surviving immunological stress. The truncated Trp biosynthetic operon, *trpRBA* (Fig. 3A), has been repeatedly linked to the ability of genital and LGV serovars (D-K and L1-3, respectively) of *C. trachomatis* to counter IFN-γ-mediated stress. This is due to the capacity of the chlamydial Trp synthase in these serovars to catalyze the β synthase reaction, *i.e.* the condensation of indole to the amino acid serine to form Trp (17). In the presence of exogenous indole, *C. trachomatis* is therefore able to biosynthesize Trp such that it can prevent the development of IFN-γ-mediated persistence. Correspondingly, the expression of *trpRBA* is highly induced following IFN-γ stimulation of infected cells (39, 40). These data have

historically implicated Trp starvation as the primary mechanism by which persistence develops in *C. trachomatis* following exposure to IFN-γ. However, these studies have routinely depended on prolonged treatment conditions that monitor the terminal effect of persistent development, as opposed to the immediate molecular events which may have important roles in the developmental fate of *Chlamydia.* As such, these studies may have missed the contribution of other IFN-γ-stimulated insults such as iron limitation.

To decouple Trp limitation from iron limitation and assess their relative contribution to regulating a critical pathway for responding to IFN-γ-mediated stress, we monitored the transcript expression of the *trpRBA* operon under brief Trp or iron starvation by RT-qPCR. When starved for Trp for 6 hrs, we observed that the expression of *trpR*, *trpB* and *trpA* were all significantly induced greater than 10.5-fold relative to 12 hpi (p = 0.00077, 0.025 and 9.7e-5, respectively; Fig. 3B). All three ORFs were also significantly elevated relative to the equivalent mock-treated time-point (p = 0.00076, 0.025 and 9.7e-5, respectively). This result was surprising with respect to the relative immediacy of operon induction in response to our Trp starvation protocol, confirming the relevant Trp-starved transcriptional phenotype. To induce Trp-deprived persistence in *C. trachomatis*, many laboratories rely on compounded techniques of IFN-γ pre-treatment to deplete host Trp pools in conjunction with culturing in Trp-depleted media, among other strategies. While the phenotypic end-point differs here, it is nonetheless interesting to note that only 6 hrs of media replacement is sufficient to markedly up-regulate *trpRBA* expression. This suggests that *C. trachomatis* has a highly attuned sensitivity to even moderate changes in Trp levels.

We next performed the same RT-qPCR analysis on the expression of the *trpRBA* operon in response to 6 hrs of iron limitation via Bpdl treatment (Fig. 3C). While we observed that the transcript expression of all three ORFs was significantly elevated at least 2.1-fold relative to the equivalent mock-treated time-point (p = 0.015, 0.00098 and 0.0062, respectively), we made the intriguing observation that only the expression *trpB* and *trpA* was significantly induced relative to 12 hpi (p = 0.00383 and 0.0195, respectively). The significant induction of *trpBA* expression, but not *trpR* expression, suggested that *trpBA* are specifically regulated by iron availability. This result is consistent with a recent survey of the iron-regulated transcriptome in *C. trachomatis* by RNA sequencing, which also reported that iron-starved *Chlamydia* specifically up-regulate *trpBA* expression in the absence of altered *trpR* expression (37). Our results expand on this finding by providing a more detailed investigation into the specific profile of this differential regulation of *trpRBA* in response to iron deprivation. Taken together, these findings demonstrated that an important stress response pathway, the *trpRBA* operon, is regulated by the availability of both Trp and iron, consistent with the notion that the pathway may be cooperatively regulated to respond to various stress conditions. Notably, iron-dependent regulation of Trp biosynthesis has not been previously documented in other prokaryotes.

Specific iron-regulated expression of *trpBA* originates from a novel alternative transcriptional start site within the *trpRBA* intergenic region. We hypothesized that the specific iron-related induction of *trpBA* expression relative to *trpR* expression may be attributable to an iron-regulated alternative transcriptional start site (alt. TSS) downstream of the *trpR* ORF. Indeed, a previous study reported the presence of an alt.

TSS in the *trpRBA* IGR, located 214 nucleotides upstream of the *trpB* translation start position (20). However, a parallel study could not identify a TrpR binding site in the *trpRBA* IGR (21). We reasoned that a similar alt. TSS may exist in the IGR that controlled the iron-dependent expression of *trpBA.* We therefore performed Rapid Amplification of 5'-cDNA Ends (5'-RACE) on RNA isolated from *C. trachomatis* L2-infected HeLa cells using the SMARTer 5'/3' RACE Kit workflow (Takara Bio). Given the low expression of the *trpRBA* operon during normal development, we utilized two sequential gene-specific amplification steps (nested 5'-RACE) to identify 5' cDNA ends in the *trpRBA* operon. These nested RACE conditions resulted in amplification that was specific to infected-cells (Fig. S3A). Using this approach, we analyzed four conditions: 12 hpi, 18 hpi, 12 hpi + 6 hrs of Bpdl treatment, and 12 hpi + 6 hrs of Trp-depletion (Fig. 4A). We observed three RACE products that migrated with an apparent size of 1.5, 1.1 and 1.0 kilobases (kb). At 12 and 18 hpi, all three RACE products exhibited low abundance, even following the nested PCR amplification. This observation was consistent with the expectation that the expression of the *trpRBA* operon is very low under normal, iron and Trp-replete conditions. However, we note that the 6-hr difference in development did appear to alter the representation of the 5' cDNA ends, which may suggest a stage-specific promoter utilization within the *trpRBA* operon. In our Trp starvation condition, we observed an apparent increase in the abundance of the 1.5 kb RACE product, which was therefore presumed to represent the primary TSS upstream of *trpR*, at nucleotide position 511,389 (*C. trachomatis* L2 434/Bu). Interestingly, the 1.0 kb product displayed a very similar apparent enrichment following Bpdl treatment, suggesting that this RACE product represented a specifically iron-regulated TSS. Both

the 1.5 and 1.0 kb RACE products were detectable in the Trp-depleted and iron-depleted conditions, respectively, during the primary RACE amplification, consistent with their induction under these conditions (Fig. S3B).

If iron depletion was inducing *trpBA* expression independent of *trpR,* we reasoned that we would observe specific enrichment of *trpB* sequences in our 5'-RACE cDNA samples relative to *trpR* sequences. We again utilized RT-qPCR to quantify the abundance of *trpB* transcripts relative to *trpR* transcripts in the 5'-RACE cDNA samples (Fig. 4B). In agreement with our model, only under iron starved conditions did we observe a significant enrichment of *trpB* relative to *trpR* ($p < 0.01$). Additionally, we observed that at 12 and 18 hpi in iron-replete conditions, the ratio of *trpB* to *trpR* was approximately 1.0, suggesting non-preferential basal expression across the three putative TSSs. Another factor contributing to this ratio is the synthesis of the full-length *trpRBA* polycistron. In support of this, the *trpB* to *trpR* ratio remained near 1.0 under the Trp-starved condition, which would be expected during transcription read-through of the whole operon. The apparent lack of preferential promoter utilization as described above could be attributed to the relatively low basal expression of the operon at 12 and 18 hpi under Trp- and iron-replete conditions, thus precluding quantitative detection of differential promoter utilization in this assay.

To determine the specific location of the 5' cDNA ends within the *trpRBA* operon, we isolated the 5'-RACE products across all conditions by gel extraction and cloned the products into the pRACE vector supplied by the manufacturer. We then sequenced the ligated inserts and BLASTed the sequences against the *C. trachomatis* L2 434/Bu genome to identify the location of the 5'-most nucleotides (Fig. 4C). These data are

displayed as a statistical approximation of the genomic regions most likely to be represented by the respective 5'-RACE products in both histogram (semi-continuous) and density plot (continuous) format (See Dataset S1 for a description of all mapped 5'-RACE products). As expected, the 1.5 kb product mapped in a distinct and tightly grouped peak near the previously annotated *trpR* TSS, with the mean and modal nucleotide being 511,388 and 511,389, respectively (Fig. S4A). Surprisingly, we found that neither the 1.1 or 1.0 kb RACE product mapped to the previously reported alt. TSS in the *trpRBA* IGR, at position 511,826. Instead, we observed that the 1.1 kb product mapped on average to nucleotide position 511,878, with the modal nucleotide being found at 511,898 (Fig. S4B). The 1.0 kb product mapped with a mean nucleotide position of 512,013, with the modal nucleotide being 512,005 (Fig. S4C), only 35 bases upstream of the *trpB* coding sequence. Interestingly, the 1.0 kb product mapped to a region of the *trpRBA* IGR flanked by consensus σ^{66} -10 and -35 promoter elements, found at positions 512,020-5 and 511,992-7, respectively (41). These data collectively pointed toward the 1.0 kb 5'-RACE product representing a novel, iron-regulated alt. TSS and *bona fide* σ^{66}-dependent promoter element that allows for the specific iron-dependent expression of *trpBA*.

YtgR specifically binds to the *trpRBA* intergenic region in an operator-dependent manner to repress transcription of *trpBA*. As the only known iron-dependent transcriptional regulator in *Chlamydia*, we hypothesized that YtgR may regulate the iron-dependent expression of *trpBA* from the putative promoter element we characterized by 5'-RACE. Using bioinformatic sequence analysis, we investigated whether the *trpRBA* IGR contained a candidate YtgR operator sequence. By local sequence alignment of

the putative YtgR operator sequence (33) and the *trpRBA* IGR, we identified a high-identity alignment (76.9% identity) covering 67% of the putative operator sequence (Fig. 5A). Interestingly, this alignment mapped to the previously identified palindrome suspected to have operator functionality (20). By global sequence alignment of the YtgR operator to the palindromic sequence, an alignment identical to the local alignment was observed, which still displayed relatively high sequence identity (43.5% identity). We hypothesized that this sequence functioned as an YtgR operator, despite being located 184 bp upstream of the *trpBA* alt. TSS.

To investigate the ability of YtgR to bind and repress transcription from the putative *trpBA* promoter, we implemented a heterologous two-plasmid assay that reports on YtgR repressor activity as a function of β-galactosidase expression (14). In brief, a candidate DNA promoter element was cloned into the pCCT expression vector between an arabinose-inducible pBAD promoter and the reporter gene *lacZ*. This plasmid was co-transformed into BL21 (DE3) *E. coli* along with an IPTG-inducible pET151 expression vector with (pET151-YtgR) or without (pET151-EV) the C-terminal 139 amino acid residues of CTL0323 (YtgC). Note that we have previously demonstrated that this region is a functional iron-dependent repressor domain (34). To verify the functionality of this assay, we determined whether ectopic YtgR expression could repress pCCT reporter gene expression in the presence of three candidate DNA elements: a no-insert empty vector (pCCT-EV), the putative promoter element for *C. trachomatis lpdA* (pCCT-*lpdA*), and the promoter region of the *ytgABCD* operon (pCCT-*ytgABCD*; Fig. 5B). As expected, from the pCCT-EV reporter construct, ectopic YtgR expression did not significantly reduce the activity of β-galactosidase. Additionally,

414 reporter gene expression from pCCT-*lpdA*, containing the promoter of iron-regulated
415 *lpdA* (37), which is not known to be YtgR-regulated, was not affected by ectopic
416 expression of YtgR. This demonstrated that the assay can discriminate between the
417 promoter elements of iron-regulated genes and *bona fide* YtgR targeted promoters.
418 Indeed, in the presence of pCCT-*ytgABCD*, induction of YtgR expression produced a
419 significant decrease in β-galactosidase activity (p = 0.03868) consistent with its
420 previously reported auto-regulation of this promoter (34).
421 Using this same assay, we then inserted into the pCCT reporter plasmid 1) the
422 *trpR* promoter element (pCCT-*trpR*), 2) the putative *trpBA* promoter element
423 represented by the IGR (pCCT-*trpBA*), and 3) the same putative *trpBA* promoter
424 element with a mutated YtgR operator sequence that was diminished for both
425 palindromicity and A-T richness, two typical features of prokaryotic promoter elements
426 (pCCT-*trpBA*ΔOperator; Fig. 5C) (42, 43). When YtgR was ectopically expressed in the
427 pCCT-*trpR* background, we observed no statistically distinguishable change in β-
428 galactosidase activity. However, in the pCCT-*trpBA* background, ectopic YtgR
429 expression significantly reduced β-galactosidase activity at levels similar to those
430 observed in the pCCT-*ytgABCD* background (p = 0.01219). This suggested that YtgR
431 was capable of binding to the *trpBA* promoter element specifically. Interestingly, this
432 repression phenotype was abrogated in the pCCT-*trpBA*ΔOperator background, where
433 we observed no statistically meaningful difference in β-galactosidase activity. We
434 subsequently addressed whether the region of the *trpRBA* IGR containing the YtgR
435 operator site was sufficient to confer YtgR repression in this assay (Fig. S5). Therefore,
436 we cloned three fragments of the *trpRBA* IGR into the pCCT reporter plasmid: the first

fragment represented the 5'-end of the IGR containing the operator site at the 3'-end (pCCT-IGR1), the second fragment represented a central region of the IGR containing the operator site at the 5'-end (pCCT-IGR2), and the third fragment represented the 3'-end of the IGR and did not contain the operator site (pCCT-IGR3). Surprisingly, we observed that none of these fragments alone were capable of producing a significant repression phenotype in our reporter system. This finding indicated that while the operator site was necessary for YtgR repression, it alone was not sufficient. Together, these data indicated that YtgR could bind to the *trpBA* promoter element and that this binding was dependent upon an intact AT-rich palindromic sequence, likely representing an YtgR operator, but that further structural elements in the *trpRBA* IGR may be necessary for repression. Nonetheless, we demonstrated the existence of a functional YtgR binding site that conferred iron-dependent transcriptional regulation to *trpBA*, independent of the major *trpR* promoter.

Iron limitation promotes transcription read-through at the *trpRBA* YtgR operator site. If YtgR binds to the operator sequence within the intergenic region under iron-replete conditions, does it influence RNA polymerase (RNAP) read-through from the major *trpR* promoter to synthesize the polycistronic *trpRBA* mRNA? We hypothesized that the presence of YtgR at the *trpRBA* operator may disadvantage the processivity of RNAP initiating transcription at the upstream *trpR* promoter. Similar systems of RNAP read-through blockage have been reported; the transcription factor Reb1p "roadblocks" RNAPII transcription read-through in yeast by a mechanism of RNAP pausing and subsequent labelling for degradation (44). To investigate this question, we first identified transcription termination sites (TTSs) in the *trpRBA* operon in *C. trachomatis.* We

460 utilized 3'-RACE to map the 3'-ends of transcripts using gene-specific primers within the
461 *trpR* CDS (Fig. 6A; bottom). We again utilized two RACE amplification cycles to
462 generate distinct, specific bands suitable for isolation and sequencing (Fig. S6B-C). By
463 gel electrophoresis of the 3'-RACE products, we observed the appearance of four
464 distinct bands that migrated with an apparent size of 0.55, 0.45, 0.40 and 0.20 kb. In our
465 Trp-depleted condition, we observed only a very weak amplification of the 2.5 – 3 kb
466 full-length *trpRBA* message by 3'-RACE (Fig. S6A). However, we did observe it across
467 all replicates. To confirm that the full-length product was relatively specific to the Trp-
468 deplete treatment, we amplified the *trpRBA* operon by RT-PCR from the 3'-RACE cDNA
469 (Fig. 6A; top). As expected, only in the Trp-deplete sample did we observe robust
470 amplification of the full-length *trpRBA* message. We note however that image contrast
471 adjustment reveals a very weak band present in all experimental samples.
472 To identify the specific TTS locations, we gel extracted the four distinct 3'-RACE
473 bands across all conditions and cloned them into the pRACE sequencing vector as was
474 done for the 5'-RACE experiments. We then sequenced the inserted RACE products
475 and mapped them to the *C. trachomatis* L2 434/Bu genome (Fig. 6B). This revealed a
476 highly dynamic TTS landscape contained almost exclusively within the *trpRBA* IGR,
477 which has not previously been investigated (For a full description of mapped 3'-RACE
478 products, see Dataset S2). The 0.20 kb RACE product mapped tightly to the 3'-end of
479 the *trpR* CDS, with a mean nucleotide position of 511,665 and a modal nucleotide
480 position of 511,667 (Fig. S7A). Contrastingly, the other three RACE products did not
481 map in such a way so as to produce specific, unambiguous modal peaks. Instead, their
482 distribution was broader and more even, with only a few nucleotide positions mapping

more than once. Accordingly, the 0.45 kb product mapped with an average nucleotide position of 511,889, just downstream of the 1.1 kb 5'-RACE product (Fig. S7C), while the 0.55 kb product mapped with an average nucleotide position of 511,986, upstream of the 1.0 kb 5'-RACE product (Fig. S7D). Interestingly, the 0.40 kb product mapped to a region directly overlapping the putative YtgR operator site, with a mean nucleotide position of 511,811 (Fig. S7B). We therefore reasoned that this putative TTS may have an iron-dependent function.

We next aimed to quantitatively analyze the possibility that iron-depletion, and thus dissociation of YtgR from this region, may facilitate transcription read-through at the operator site. Working from the 3'-RACE generated cDNAs, we utilized RT-qPCR to monitor the abundance of various amplicons across the *trpRBA* operon in relation to a "read-through" normalization amplicon that should only be represented when the full-length *trpRBA* message is transcribed (Fig. 6C). Therefore, as each amplicon is increasingly represented as a portion of the full-length, read-through transcript, the representation ratio of the specific amplicon to the normalization amplicon should approach 1.0. We first analyzed an amplicon from nucleotide 511,416 – 531 to monitor transcript species associated with transcription initiating at the *trpR* promoter. We observed that the representation of this amplicon was not significantly altered following iron limitation relative to 12 hpi, suggesting that the depletion of iron was not affecting initiation of transcription at the *trpR* promoter. Interestingly, at 18 hpi, the representation ratio of this amplicon significantly shifted further away from 1.0 (p = 0.00358), indicating that at 18 hpi this amplicon is represented less as a component of read-through transcription relative to 12 hpi. As expected, under Trp-deplete conditions, the

representation ratio shifted significantly closer to 1.0 (p = 0.00064), consistent with read-through transcription of the full-length *trpRBA* message.

We then preformed the same analysis on an amplicon from nucleotide 511,639 – 764, immediately upstream of the TTS at the YtgR operator site. We again observed that at 18 hpi, the representation ratio was significantly increased (p = 0.01046), and following Trp-depletion, the ratio was significantly decreased (p = 0.00023), as expected. Notably, and consistent with our hypothesis, we observed that the representation ratio of this amplicon was also significantly closer to 1.0 following iron limitation (p = 0.00407), suggesting that transcription read-through was increased at this site under iron limited conditions. If YtgR is dissociating from the operator site during iron depletion, a greater proportion of transcripts would be expected to read-through this locus.

Finally, we analyzed an amplicon from nucleotide 513,856 – 968, at the very 3'-end of *trpA* to monitor terminal transcription under our experimental conditions. At 18 hpi, we observed a significant increase in the representation ratio of this amplicon (p = 0.00476), which is likely attributable to both basal levels of alternative transcription from the IGR as well as poor transcription read-through of the full-length message. Following 6 hrs of Bpdl treatment, we also observed a significant increase in the representation ratio of this amplicon (p = 0.01510), which supports the finding that *trpBA* is being preferentially transcribed under this condition, distinct from the full-length *trpRBA* transcript. We were only able to detect a marginal decrease in the representation of this amplicon under Trp-depleted conditions (p = 0.07942), which may suggest that the very 3'-end of *trpRBA* is relatively under-represented than our normalization amplicon, which

529 falls within the middle of the operon. In fact, recent work has reported on the relatively
530 poor representation of 3'-end mRNAs in *Chlamydia* (45). In sum, this set of experiments
531 provides evidence that iron-depletion specifically alters the representation of particular
532 mRNA species across the *trpRBA* operon. Additionally, they implicate iron-dependent
533 YtgR DNA-binding as the mediator of these effects. By alleviating YtgR repression via
534 iron depletion, transcription is allowed to proceed through the operator site, albeit at
535 basal levels. Concomitantly, transcription is specifically activated at the downstream alt.
536 TSS for *trpBA*.

537 **Discussion**

538 In this study, we report a mechanism of stress adaptation that integrates
539 responses to iron and Trp starvation. Specifically, we demonstrated that the *trpRBA*
540 operon is transcriptionally regulated by the iron-dependent repressor YtgR. We
541 determined that iron-dependent expression of *trpBA* initiates from a novel internal
542 promoter in an IGR of the *trpRBA* operon and that this IGR also contains an YtgR
543 operator site necessary to confer a transcriptional repression phenotype. We suggest
544 that the dual promoter configuration of *trpRBA* presents the opportunity for YtgR to
545 block transcription read-through from the *trpR* promoter; transcripts terminate at the
546 YtgR operator site and iron depletion facilitates read-through of the operon at this locus.
547 This is the first time an iron-dependent mode of regulation has been shown to control
548 the expression of tryptophan biosynthesis in prokaryotes, which is a reflection of the
549 uniquely specialized nature of *C. trachomatis*.

550 The distance separating the YtgR operator site from the *trpBA* alt. TSS indicate
551 the involvement of a regulatory mechanism more complex than simple steric hindrance

of RNAP by YtgR. One possible explanation is that YtgR functions similarly to other prokaryotic transcription factors that repress “at a distance” by a mechanism of DNA-bending (46, 47). In this scenario, YtgR binding simultaneously to an additional operator site may facilitate a conformational bend in the double-helix DNA such that RNAP no longer has access to the alternative *trpBA* promoter site. This would be consistent with the observation that a truncated *trpRBA* IGR containing the candidate YtgR operator is insufficient to confer transcriptional repression. The topological alteration induced by DNA-bending could also feasibly contribute to diminished RNAP read-through from the *trpR* promoter. *In silico* identification of additional putative YtgR operator sites was unsuccessful, which could be due to the lack of enough validated binding sites to generate a robust consensus sequence. Thus, a more unbiased approach (*e.g.* ChIP-Sequencing) will be required to identify additional YtgR binding events. We also note that the YtgR operator upstream of *ytgA*, while only 21 bp from the predicted -35 element, rests within a 660-bp IGR, raising the possibility that other cryptic YtgR operators are present in this sequence. Another possibility is that YtgR functions in concert with additional transcription factors more proximal to the *trpBA* promoter elements. In *E. coli*, the repressor Fis binds 135 bp upstream of the *nir* promoter TSS, controlling co-activation of *nir* expression by proximally-bound Fnr and NarL/NarP (48). While we have no evidence to suggest other transcription factors are controlling *trpBA* expression, this does not preclude the possibility of their involvement.

While we demonstrate here that iron-dependent *trpBA* expression originates from a novel promoter element immediately upstream of the *trpB* CDS, this is not the first description of an alt. TSS within the *trpRBA* IGR. Carlson, et al. identified an alt. TSS

within the IGR which they suggested was responsible for *trpBA* expression (20). Interestingly, this TSS was observed to originate from within the palindromic sequence that we have identified here as a functional YtgR operator site. In these studies, we were unable to confirm the presence of the previously identified alt. TSS by 5'-RACE. This is likely because Carlson, et al. examined the presence of transcript origins following 24 hrs of Trp starvation whereas here we monitored immediate responses to stress following only 6 hrs of treatment. Prolonged Trp depletion would result in a more homogeneously stressed population of chlamydial organisms that may exhibit the same preferential utilization of the promoter identified by Carlson, et al. Population heterogeneity in response to brief stress may explain the observation of multiple T(S/T)Ss across the *trpRBA* operon in our studies. However, the contribution of such a Trp-dependent alt. TSS to the general stress response of *C. trachomatis* remains unclear. Akers & Tan were unable to verify TrpR binding to the *trpRBA* IGR by EMSA, suggesting that some other Trp-dependent mechanism may control transcription from this site (21). Ultimately, our approach of investigating more immediate responses to stress revealed previously unreported mechanisms functioning to regulate Trp biosynthesis in *C. trachomatis*, underscoring the value of transient as opposed to sustained induction of stress.

Another mechanism of regulation reported to control the chlamydial *trpRBA* operon is Trp-dependent transcription attenuation. Based on sequence analysis, a leader peptide has been annotated within the *trpRBA* IGR (23). Presumably, this functions analogously to the attenuator in the *E. coli trpEDCBA* operon; Trp starvation causes ribosome stalling at sites of enriched Trp codons such that specific RNA

598 secondary structures form to facilitate RNAP read-thru of downstream sequences – in
599 this case, *trpBA* (49). However, robust experimental evidence to support the existence
600 of attenuation in *C. trachomatis* is lacking. To date, the only experimental evidence that
601 supports this model was reported by Carlson, et al., who demonstrated that transcript
602 expression of *trpBA* is increased following 24 hr Trp-depletion in a *trpR*-mutant strain of
603 *C. trachomatis*, suggesting that an additional level of Trp-dependent regulation controls
604 *trpBA* expression (20). However, this could be attributable to an alternative Trp-
605 dependent mechanism controlling *trpBA* expression at the alt. TSS identified by
606 Carlson, et al. None of the data presented here point conclusively to the existence of a
607 Trp-dependent attenuator; while we acknowledge that the additional termination sites
608 identified in our 3'-RACE assay may represent termination events mediated by an
609 attenuator, without more specific analysis utilizing mutated sequences we cannot draw
610 definitive conclusions about the functional relevance of those termination sites.
611 Additionally, it is unlikely that we would be able to observe Trp-dependent attenuation
612 under our brief stress conditions given that attenuation has a much higher tolerance for
613 Trp-depletion than TrpR-mediated transcriptional repression in *E. coli* (50).
614 Interestingly, in *Bacillus subtilis,* Trp-dependent attenuation of transcription takes
615 on a form markedly different from that in *E. coli*. Whereas attenuation functions in *cis* for
616 the *E. coli trp* operon, *B. subtilis* utilize a multimeric Tryptophan-activated RNA-binding
617 Attenuation Protein, TRAP, which functions in *trans* to bind *trp* operon RNA under Trp-
618 replete conditions, promoting transcription termination and inhibiting translation (51).
619 This interaction is antagonized by anti-TRAP in the absence of charged $tRNA^{Trp}$, leading
620 to increased expression of TRAP regulated genes. We suggest that YtgR may

represent the first instance of a separate and distinct clade of attenuation mechanisms: iron-dependent *trans*-attenuation. We have demonstrated that transcription terminates in the *trpRBA* operon at the YtgR operator site, and that read-thru of the operon is facilitated under iron-deplete conditions, which is consistent with the idea that relief of iron-activated YtgR DNA-binding at this site would permit RNAP to pass through the YtgR operator site. This mechanism may function independently of specific RNA secondary structure, relying instead on steric blockage of RNAP processivity, but ultimately producing a similar result. Possible regulation of translation remains to be explored. The recent development of new genetic tools to alter chromosomal sequences and generate conditional knockouts in *C. trachomatis* should enable a more detailed analysis of *trpRBA* regulation, including possible *trans*-attenuation (52, 53).

As a Trp auxotroph, what might be the biological significance of iron-dependent YtgR regulation of the *trpRBA* operon in *C. trachomatis*? We have already noted the possibility that iron-dependent *trpBA* regulation in *C. trachomatis* may enable a response to simultaneous Trp and iron starvation, such as that likely mediated by IFN-γ. However, this mechanism also presents the opportunity for *C. trachomatis* to respond similarly to distinct *sequential* stresses, where a particular stress primes the pathogen to better cope with subsequent stresses. To reach the female upper genital tract (UGT), where most significant pathology is identified following infection with *C. trachomatis*, the pathogen must first navigate the lower genital tract (LGT). *Chlamydia* infections of the female LGT are associated with bacterial vaginosis (BV), which is characterized by obligate and facultative anaerobe colonization, some of which catalyze the production of indole (54, 55). This provides *C. trachomatis* with the necessary substrate to salvage

644 tryptophan via TrpBA. Interestingly, the LGT is also likely an iron-limited environment.
645 Pathogen colonization and BV both increase the concentration of mucosal lactoferrin
646 (Lf), an iron-binding glycoprotein, which can starve pathogens for iron (56, 57). Lf
647 expression is additionally hormone-regulated, and thus the LGT may normally
648 experience periods of iron limitation (58, 59). Moreover, the expression of TfR is
649 constrained to the basal cells of the LGT stratified squamous epithelium (60), which
650 likely restricts iron from *C. trachomatis* infecting the accessible upper layers of the
651 stratified epithelia. In fact, it was recently demonstrated that *C. trachomatis*
652 development is attenuated in the terminally differentiated layers of an *in vitro*-generated
653 stratified squamous epithelium (61). Collectively, LGT conditions that favor *C.*
654 *trachomatis* infection may be marked by concomitant iron limitation and indole
655 accessibility. For *C. trachomatis*, iron limitation may therefore serve as a critical signal in
656 the LGT, inducing the expression of *trpBA* such that Trp is stockpiled from available
657 indole, allowing the pathogen to counteract oncoming IFN-γ-mediated Trp starvation.
658 We propose the possibility that iron limitation in the LGT may be a significant predictor
659 of pathogen colonization in the UGT.
660 Finally, and of note, the expression of the ribonucleotide diphosphate-reductase
661 encoding *nrdAB* was also recently shown to be iron-regulated in *C. trachomatis* (37).
662 The regulation of *nrdAB* is known to be mediated by the presumably
663 deoxyribonucleotide-dependent transcriptional repressor NrdR, encoded distal to the
664 *nrdAB* locus (62). As NrdR activity is not known to be modulated by iron availability, this
665 raises the intriguing possibility that here too a unique iron-dependent mechanism of
666 regulation may integrate the chlamydial stress response to promote a unified response

667 across various stress conditions. Future studies may require more metabolomics-based
668 approaches to thoroughly dissect the integration of these stress responses, as
669 transcriptome analyses alone often miss broader, pathway-oriented metabolic
670 coordination. Ultimately, these studies point towards a need to carefully re-evaluate the
671 molecular stress response in *Chlamydia*, using more targeted approaches to answer
672 more specific questions. We anticipate that the rapid progress of the field in recent
673 years will continue to catalyze exciting and important discoveries regarding the
674 fundamental biology of *Chlamydia*.

675 **Materials and Methods**

676 Please refer to the *SI Appendix* for a complete and detailed description of all
677 experimental reagents and methodology. For all infections, *Chlamydia trachomatis* LGV
678 serological variant type II was used to infect human cervical epithelial adenocarcinoma
679 HeLa cells at a multiplicity of infection of 2 or 5, depending on experiment. Indirect
680 immunofluorescent confocal microscopy experiments were performed on a Leica TCS
681 SP8 laser scanning confocal microscope in the Integrative Physiology and
682 Neuroscience Advanced Imaging Center at Washington State University. RT-qPCR and
683 qPCR experiments were performed essentially as described (35, 37). Transcript
684 abundance was normalized to genome copy number for all RT-qPCR analyses. RACE
685 experiments were conducted using the SMARTer® RACE 5'/3' Kit (Takara Bio) with
686 minor modifications as noted in *SI Materials and Methods*. RACE products were
687 isolated by gel extraction using the Macherey-Nagel Nucleospin PCR/gel clean-up kit
688 (Takara Bio) and sent to Eurofins Genomics, LLC for sequencing. Sequenced RACE
689 products were mapped to the *C. trachomatis* L2 434/Bu genome (NCBI Accession:

690 NC_010287) by nucleotide BLAST on the NCBI server. The *E. coli* YtgR reporter assay
691 was performed essentially as described (34) with minor modifications as indicated in *SI*
692 *Materials and Methods.* Briefly, BL21 (DE3) *E. coli* were co-transformed with the
693 indicated pCCT and pET vectors and clonal populations were selected on double-
694 selective media. Clones were cultured in double-selective media and recombinant YtgR
695 expression was induced by the addition of IPTG prior to induction of *lacZ* expression by
696 the addition of L-arabinose. Cell lysates were collected and β-galactosidase activity was
697 measured by the Miller Assay (63).

698 **Acknowledgements.** We thank Dr. Amanda Brinkworth, Liam Caven, Korinn Murphy
699 and Matthew Romero for critical review of this manuscript; Christopher C. Thompson for
700 the establishment of the *E. coli* YtgR reporter system and generation of the pCCT
701 construct; Dr. David Dewitt for expert advice, training and maintenance of equipment in
702 the IPN Advanced Imaging Center. This work was supported by NIH grants 5RO1-
703 AI065545-07 to R.A.C.; 1F31AI136295-01A1 and 5T32GM008336-29 to N.D.P.; N.D.P.
704 was also supported by an Achievement Reward for College Scientists (ARCS; Seattle
705 Chapter) Fellowship.

706 **References**

707 1. Skaar EP (2010) The battle for iron between bacterial pathogens and their
708 vertebrate hosts. *PLoS Pathog* 6(8):1–2.
709 2. Eisenreich W, Dandekar T, Heesemann J, Goebel W (2010) Carbon metabolism
710 of intracellular bacterial pathogens and possible links to virulence. *Nat Rev*
711 *Microbiol* 8(6):401–412.
712 3. Brown SA, Palmer KL, Whiteley M (2008) Revisiting the host as a growth

713 medium. *Nat Rev Microbiol* 6(9):657–666.

714 4. Ray K, Marteyn B, Sansonetti PJ, Tang CM (2009) Life on the inside: The
715 intracellular lifestyle of cytosolic bacteria. *Nat Rev Microbiol* 7(5):333–340.

716 5. Hood MI, Skaar EP (2012) Nutritional immunity: Transition metals at the
717 pathogen-host interface. *Nat Rev Microbiol* 10(8):525–537.

718 6. CDC (2017) *2016 Sexually Transmitted Diseases Surveillance - Chlamydia*
719 Available at: https://www.cdc.gov/std/stats16/chlamydia.htm.

720 7. Taylor HR, Burton MJ, Haddad D, West S, Wright H (2014) Trachoma. *Lancet*
721 384(9960):2142–2152.

722 8. Newman L, et al. (2015) Global Estimates of the Prevalence and Incidence of
723 Four Curable Sexually Transmitted Infections in 2012 Based on Systematic
724 Review and Global Reporting. *PLoS One* 10(12):1–17.

725 9. Hafner LM (2015) Pathogenesis of fallopian tube damage caused by Chlamydia
726 trachomatis infections. *Contraception* 92(2):108–115.

727 10. Moore ER, Ouellette SP (2014) Reconceptualizing the chlamydial inclusion as a
728 pathogen-specified parasitic organelle: an expanded role for Inc proteins. *Front*
729 *Cell Infecit Microbiol* 4(October):1–10.

730 11. AbdelRahman YM, Belland RJ (2005) The chlamydial developmental cycle.
731 *FEMS Microbiol Rev* 29(5):949–959.

732 12. Clarke IN (2011) Evolution of Chlamydia trachomatis. *Ann N Y Acad Sci* 1230:11–
733 18.

734 13. Stephens RS, et al. (1998) Genome sequence of an obligate intracellular
735 pathogen of humans: Chlamydia trachomatis. *Science (80-)* 282(5389):754–759.

14. Wyrick PB (2010) Chlamydia trachomatis Persistence In Vitro: An Overview. *J Infect Dis* 201:88–95.

15. Byrne GI, Lehmann LK, Landry GJ (1986) Induction of tryptophan catabolism is the mechanism for gamma-interferon-mediated inhibition of intracellular Chlamydia psittaci replication in T24 cells. *Infect Immun* 53(2):347–351.

16. Taylor MW, Feng GS (1991) Relationship between interferon-gamma, indoleamine 2,3-dioxygenase, and tryptophan catabolism. *FASEB J* 5(11):2516–2522.

17. Fehlner-Gardiner C, et al. (2002) Molecular basis defining human Chlamydia trachomatis tissue tropism: A possible role for tryptophan synthase. *J Biol Chem* 277(30):26893–26903.

18. Macchiarulo A, Camaioni E, Nuti R, Pellicciari R (2009) Highlights at the gate of tryptophan catabolism□: a review on the mechanisms of activation and regulation of indoleamine 2,3-dioxygenase (IDO), a novel target in cancer disease. *Amino Acids* 37:219–229.

19. Wood H, Roshick C, McClarty G (2004) Tryptophan recycling is responsible for the interferon-? resistance of Chlamydia psittaci GPIC in indoleamine dioxygenase-expressing host cells. *Mol Microbiol* 52(3):903–916.

20. Carlson JH, Wood H, Roshick C, Caldwell HD, McClarty G (2006) In vivo and in vitro studies of Chlamydia trachomatis TrpR:DNA interactions. *Mol Microbiol* 59(6):1678–1691.

21. Akers JC, Tan M (2006) Molecular mechanism of tryptophan-dependent transcriptional regulation in Chlamydia trachomatis. *J Bacteriol* 188(12):4236–

4243.

22. Wood H, et al. (2003) Regulation of tryptophan synthase gene expression in Chlamydia trachomatis. *Mol Microbiol* 49(5):1347–1359.

23. Merino E, Yanofsky C (2005) Transcription attenuation: A highly conserved regulatory strategy used by bacteria. *Trends Genet* 21(5):260–264.

24. Cassat JE, Skaar EP (2013) Iron in Infection and Immunity. *Cell Host Microbe* 13(5):509–519.

25. Raulston JE (1997) Response of Chlamydia trachomatis serovar E to iron restriction in vitro and evidence for iron-regulated chlamydial proteins. *Infect Immun* 65(11):4539–4547.

26. Ouellette SP, Carabeo RA (2010) A functional slow recycling pathway of transferrin is required for growth of Chlamydia. *Front Microbiol* 1(OCT):1–12.

27. Igietseme JU, Ananaba GA, Candal DH, Lyn D, Black CM (1998) Immune control of Chlamydial growth in the human epithelial cell line RT4 involves multiple mechanisms that include nitric oxide induction, tryptophan catabolism and iron deprivation. *Microbiol Immunol* 42(9):617–625.

28. Nairz M, et al. (2008) Interferon-γ limits the availability of iron for intramacrophage Salmonella typhimurium. *Eur J Immunol* 38(7):1923–1936.

29. Byrd T, Horwitz MA (1989) Interferon gamma-activated human monocytes downregulate transferrin receptors and inhibit the intracellular multiplication of Legionella pneumophila by limiting the availability of iron. *J Clin Invest* 83(5):1457–1465.

30. Byrd TF, Horwitz MA (1993) Regulation of transferrin receptor expression and

ferritin content in human mononuclear phagocytes: Coordinate upregulation by iron transferrin and downregulation by interferon gamma. *J Clin Invest* 91(3):969–976.

31. Pokorzynski ND, Thompson CC, Carabeo RA (2017) Ironing Out the Unconventional Mechanisms of Iron Acquisition and Gene Regulation in Chlamydia. *Front Cell Infect Microbiol* 7(September):1–19.

32. Miller JD, Sal MS, Schell M, Whittimore JD, Raulston JE (2009) Chlamydia trachomatis YtgA is an iron-binding periplasmic protein induced by iron restriction. *Microbiology* 155(9):2884–2894.

33. Akers JC, HoDac H, Lathrop RH, Tan M (2011) Identification and functional analysis of CT069 as a novel transcriptional regulator in Chlamydia. *J Bacteriol* 193(22):6123–6131.

34. Thompson CC, Nicod SS, Malcolm DS, Grieshaber SS, Carabeo RA (2012) Cleavage of a putative metal permease in Chlamydia trachomatis yields an iron-dependent transcriptional repressor. *Proc Natl Acad Sci U S A* 109(26):10546–51.

35. Thompson CC, Carabeo RA (2011) An optimal method of iron starvation of the obligate intracellular pathogen, Chlamydia trachomatis. *Front Microbiol* 2(20). doi:10.3389/fmicb.2011.00020.

36. Dill BD, Dessus-Babus S, Raulston JE (2009) Identification of iron-responsive proteins expressed by Chlamydia trachomatis reticulate bodies during intracellular growth. *Microbiology* 155(1):210–219.

37. Brinkworth AJ, Wildung MR, Carabeo RA (2018) Genomewide Transcriptional Responses of Iron-Starved Chlamydia trachomatis Reveal Prioritization of

Metabolic Precursor Synthesis over Protein Translation. *mSystems* 3(1):e00184-17.

38. Raulston JE, et al. (2007) Identification of an iron-responsive protein that is antigenic in patients with Chlamydia trachomatis genital infections. *FEMS Immunol Med Microbiol* 51(3):569–576.

39. Belland RJ, et al. (2003) Transcriptome analysis of chlamydial growth during IFN-gamma-mediated persistence and reactivation. *Proc Natl Acad Sci U S A* 100(26):15971–15976.

40. Østergaard O, et al. (2016) Quantitative Protein Profiling of Chlamydia trachomatis Growth Forms Reveals Defense Strategies Against Tryptophan Starvation. *Mol Cell Proteomics* 15(12):3540–3550.

41. Ricci S, Ratti G, Scarlato V (1995) Transcriptional regulation in the Chlamydia trachomatis pCT plasmid. *Gene* 154(1):93–98.

42. Tao X, Boydt J, Murphy JR (1992) Specific binding of the diphtheria tox regulatory element DtxR to the tox operator requires divalent heavy metal ions and a 9-base-pair interrupted palindromic sequence. *Proc Natl Acad Sci U S A* 89(13):5897–5901.

43. Schmitt MP (2002) Analysis of a DtxR-Like Metalloregulatory Protein, MntR, from Corynebacterium diphtheriae That Controls Expression of an ABC Metal Transporter by an Mn(2+)-Dependent Mechanism. *J Bacteriol* 184(24):6882–6892.

44. Colin J, et al. (2014) Roadblock termination by reb1p restricts cryptic and readthrough transcription. *Mol Cell* 56(5):667–680.

828 45. Ouellette SP, Rueden KJ, Rucks EA (2016) Tryptophan codon-dependent
829 transcription in chlamydia pneumoniae during gamma interferon-mediated
830 tryptophan limitation. *Infect Immun* 84(9):2703–2713.
831 46. Gralla JD (1989) Bacterial gene regulation from distant DNA sites. *Cell* 57(2):193–
832 195.
833 47. Sankar A (1989) Multipartite genetic control elements: communication by DNA
834 loop. *Annu Rev Genet* 23(53):227–250.
835 48. Wu HC, Tyson KL, Cole JA, Busby SJW (1998) Regulation of transcription
836 initiation at the Escherichia coli nir operon promoter: A new mechanism to
837 account for co-dependence on two transcription factors. *Mol Microbiol* 27(2):493–
838 505.
839 49. Yanofsky C (1981) Attenuation in the control of expression of bacterial operons.
840 *Nature* 289(5800):751–758.
841 50. Yanofsky C, Kelley RL, Horn V (1984) Repression is relieved before attenuation in
842 the trp operon of Escherichia coli as tryptophan starvation becomes increasingly
843 severe. *J Bacteriol* 158(3):1018–1024.
844 51. Gollnick P, Babitzke P, Antson A, Yanofsky C (2005) Complexity in regulation of
845 tryptophan biosynthesis in Bacillus subtilis. *Annu Rev Genet* 39(October):47–68.
846 52. Mueller KE, Wolf K, Fields KA (2016) Gene Deletion by Fluorescence-Reported
847 Allelic Exchange Mutagenesis in Chlamydia trachomatis. 7(1):1–9.
848 53. Ouellette SP (2018) Feasibility of a Conditional Knockout System for Chlamydia
849 Based on CRISPR Interference. *Front Cell Infect Microbiol* 8(February).
850 doi:10.3389/fcimb.2018.00059.

54. Sasaki-Imamura T, Yoshida Y, Suwabe K, Yoshimura F, Kato H (2011) Molecular basis of indole production catalyzed by tryptophanase in the genus Prevotella. *FEMS Microbiol Lett* 322(1):51–59.

55. Ziklo N, Huston WM, Hocking JS, Timms P (2016) Chlamydia trachomatis Genital Tract Infections: When Host Immune Response and the Microbiome Collide. *Trends Microbiol* 24(9):750–765.

56. Valenti P, et al. (2018) Role of Lactobacilli and Lactoferrin in the Mucosal Cervicovaginal Defense. *Front Immunol* 9(March):1–14.

57. Spear GT, et al. (2011) Multiplex immunoassay of lower genital tract mucosal fluid from women attending an urban STD clinic shows broadly increased IL1ß and lactoferrin. *PLoS One* 6(5):1–7.

58. Kelver ME, et al. (1996) Estrogen regulation of lactoferrin expression in human endometrium. *Am J Reprod Immunol* 36(5):243–247.

59. Cohen M, Britigan B, French M, Bean K (1987) Preliminary observations on lactoferrin secretion in human vaginal mucus: variation during the menstrual cycle, evidence of hormonal regulation, and implications for infection with Neisseria gonorrhoeae. *Am J Obstet Gynecol* 157(5):1122–1125.

60. Lloyd JM, O'Dowd T, Driver M, Tee DE (1984) Demonstration of an epitope of the transferrin receptor in human cervical epithelium--a potentially useful cell marker. *J Clin Pathol* 37(2):131–135.

61. Nogueira AT, Braun KM, Carabeo RA (2017) Characterization of the Growth of Chlamydia trachomatis in In Vitro-Generated Stratified Epithelium. *Front Cell Infect Microbiol* 7(October):1–16.

874 62. Case EDR, Akers JC, Tan M (2011) CT406 encodes a chlamydial ortholog of
875 NrdR, a repressor of ribonucleotide reductase. *J Bacteriol* 193(17):4396–4404.
876 63. Miller JH (1972) Assay of β-galactosidase. *Experiments in Molecular Genetics*
877 (Cold Spring Harbor Laboratory Press).

878 **Figure Legends**

879 **Fig. 1.** Brief iron limitation via 2,2-bipyridyl treatment precedes the onset of
880 characteristic chlamydial persistence. (*A*) *C. trachomatis* L2-infected HeLa cells were
881 fixed and stained with convalescent human sera to image inclusion morphology by
882 confocal microscopy following Bpdl treatment at the indicated times post-infection.
883 Arrowheads indicate inclusions with visibly fewer organisms in the 12-hour Bpdl-treated
884 condition. Figure shows representative experiment of three biological replicates. (*B*)
885 Genomic DNA (gDNA) was harvested from infected HeLa cells at the indicated times
886 post-infection under iron-replete (blue) and -deplete (red) conditions. Chlamydial
887 genome copy number was quantified by qPCR. Chlamydial genome replication is
888 stalled following 12 hours of Bpdl treatment, but not 6. N=2. (*C*) Total RNA was
889 harvested from infected HeLa cells at the indicated times post-infection under iron-
890 replete (teal) and -deplete (orange) conditions. The transcript abundance of hallmark
891 persistence genes *euo* and (*D*) *omcB* were quantified by RT-qPCR and normalized
892 against genome copy number. Only at 12 hours of Bpdl treatment is *omcB* expression
893 significantly affected. N=3 for 12+6, N=2 for 12+12. Statistical significance was
894 determined by One-Way ANOVA followed by post-hoc pairwise *t*-tests with Bonferroni's
895 correction for multiple comparisons. * = $p < 0.05$, ** = $p < 0.01$, *** = $p < 0.005$.
896

Fig. 2. Brief iron limitation condition produces mild iron-starved transcriptional phenotype. (*A*) Total RNA and gDNA was harvested from infected HeLa cells at the indicated times post-infection under iron-replete (teal) and -deplete (orange) conditions. The transcript abundance of iron-regulated *ytgA,* (*B*) *ahpC,* (*C*) *devB* and (*D*) non-iron regulated *dnaB* were quantified by RT-qPCR and normalized against genome copy number. The transcript expression of *ytgA* and *ahpC* were significantly elevated following 6-hour Bpdl treatment, indicative or iron starvation to *C. trachomatis.* N=3. Statistical significance was determined by One-Way ANOVA followed by post-hoc pairwise *t*-tests with Bonferroni's correction for multiple comparisons. * = $p < 0.05$, ** = $p < 0.01$, *** = $p < 0.005$.

Fig. 3. Expression of the *trpRBA* operon in *C. trachomatis* is non-uniformly regulated by brief iron limitation. (*A*) Cartoon depiction of the *trpRBA* operon (drawn to scale) with the primary transcriptional start site upstream of *trpR* annotated. (*B*) Total RNA and gDNA were harvested from infected HeLa cells at the indicated times post-infection under Trp-replete (black) and -deplete (red) conditions. The transcript expression of *trpRBA* operon was quantified by RT-qPCR and normalized against genome copy number. All three ORFs are significantly induced relative to 12 hpi following Trp starvation. N=2. (*C*) Total RNA and gDNA were harvested from infected HeLa cells at the indicated times post-infection under iron-replete (blue) and -deplete (red) conditions. The transcript expression of *trpRBA* operon was quantified by RT-qPCR and normalized against genome copy number. Only *trpB* and *trpA* expression was significantly induced relative to 12 hpi. N=3. Statistical significance was determined by One-Way ANOVA followed by

post-hoc pairwise *t*-tests with Bonferroni's correction for multiple comparisons. * = $p < 0.05$, ** = $p < 0.01$, *** = $p < 0.005$.

Fig. 4. Iron-dependent induction of *trpBA* expression initiates within the *trpRBA* intergenic region from a novel alternative transcriptional start site. (*A*) Total RNA was harvested from infected HeLa cells at the indicated times post-infection to examine iron-dependent and Trp-dependent changes in the 5'-cDNA profile of the *trpRBA* operon by Rapid Amplification of 5' cDNA Ends (5'-RACE). RACE products were separated on an agarose gel, revealing three distinct and specific bands with apparent sizes of 1.5, 1.1 and 1.0 kb. Trp depletion led to the apparent enrichment of the 1.5 kb product, while Bpdl treatment produced a similarly enriched 1.0 kb RACE product. Figure shows representative experiment of three biological replicates. (*B*) To confirm that iron-dependent induction of *trpBA* could originate from alternative transcription initiation, RT-qPCR was performed on 5'-RACE cDNA to quantify the abundance of *trpB* transcripts relative to *trpR.* Only under iron-limited conditions were *trpB* transcripts enriched relative to *trpR*. N=3. Statistical significance determined by One-way ANOVA followed by post-hoc pairwise *t*-tests. * = $p < 0.05$, ** = $p < 0.01$, *** = $p < 0.005$. (*C*) The nucleotide position of the 5' cDNA ends generated from RACE were mapped to the *C. trachomatis* L2 434/Bu genome by nucleotide BLAST. Figure displays histogram (discrete; bin width=20) and overlaid density plot (continuous) distribution of 5' nucleotide positions generated from each 5'-RACE product. The dotted line represents the weighted mean of the distribution, as indicated by the integer value above each line. The identified alt. TSSs are depicted on the *trpRBA* operon (drawn to scale) above the plot. N=3.

943

944 **Fig. 5.** Ectopically expressed YtgR domain is capable of binding the putative *trpBA*
945 promoter element in an operator-specific manner and repress transcription in a
946 heterologous system. (*A*) Identification of putative YtgR operator sequence by local and
947 global nucleotide sequence alignment using EMBOSS Water and Needle algorithms,
948 respectively, to align the previously identified YtgR operator to both the *trpRBA* IGR and
949 palindromic candidate sequence. The palindrome was then mutated in our YtgR
950 repression assay as depicted to abolish palindromicity and AT-richness. (*B*) Ectopic
951 expression of YtgR significantly represses β-galactosidase activity only from the
952 promoter of its own operon, *ytgABCD*, and not from an empty vector or another iron-
953 regulated but presumably non-YtgR targeted promoter, *lpdA.* $3 \leq N \geq 2$. (*C*) Expression
954 of recombinant YtgR represses β-galactosidase activity from the putative *trpBA*
955 promoter element, but not the *trpR* promoter, and this repression is dependent on the
956 unaltered operator sequence identified in Fig. 5A. $3 \leq N \geq 2$. Statistical significance
957 determined by two-sided unpaired Student's *t*-test with Welch's correction for unequal
958 variance. * = $p < 0.05$, ** = $p < 0.01$, *** = $p < 0.005$.

959

960 **Fig. 6.** Transcription termination at *trpRBA* YtgR operator site coincides with iron-
961 dependent transcription read-through. (*A*) Total RNA was harvested from *C.*
962 *trachomatis*-infected HeLa cells to analyze 3'-cDNA landscape downstream of *trpR*
963 promoter. The top panel displays representative RT-PCR of full-length *trpRBA* message
964 across experimental conditions (NTC = No Template Control). Bottom panel depicts
965 electrophoresed 3'-RACE products and estimated sizes. N=3. (*B*) 3'-RACE products

were sequenced and mapped to *C. trachomatis* L2 434/Bu genome by nucleotide BLAST. The 0.40 kb RACE product mapped to a region overlapping the predicted YtgR operator site, as indicated by the cartoon depiction of the *trpRBA* operon (drawn to scale) above the plot. N=3. (*C*) Analysis of transcription read-through by RT-qPCR was performed on 3'-RACE cDNAs at three distinct loci across the *trpRBA* operon representing upstream transcription initiation (511,416-531), YtgR operator site termination (511,639-764) and terminal *trpBA* transcription (513,856-968). Abundance of each amplicon was normalized to a region (Read-through) predicted to be transcribed only as a part of the full-length product based on 5' and 3'-RACE data (511,792-512,080). Thus, the ratio of each amplicon to the normalization amplicon represents the proportion of that amplicon encoded as part of the full-length transcript, approaching one as the two more closely coincide. At the YtgR operator termination site, iron limitation reduces the ratio relative to 12 hpi, suggesting that transcription read-through increases at this site under this condition. The transcription initiation ratio is unaffected by iron limitation, while the terminal *trpBA* amplicon is increased, consistent with alternative transcription from the alt. TSS. Statistical significance determined by One-way ANOVA followed by post-hoc pairwise *t*-tests. * = $p < 0.05$, ** = $p < 0.01$, *** = $p < 0.005$.

Author Contributions: N.D.P. and R.A.C. wrote the manuscript; N.D.P. and R.A.C. designed the experiments; N.D.P. performed the experiments; N.D.P. and R.A.C. analyzed and interpreted the data.

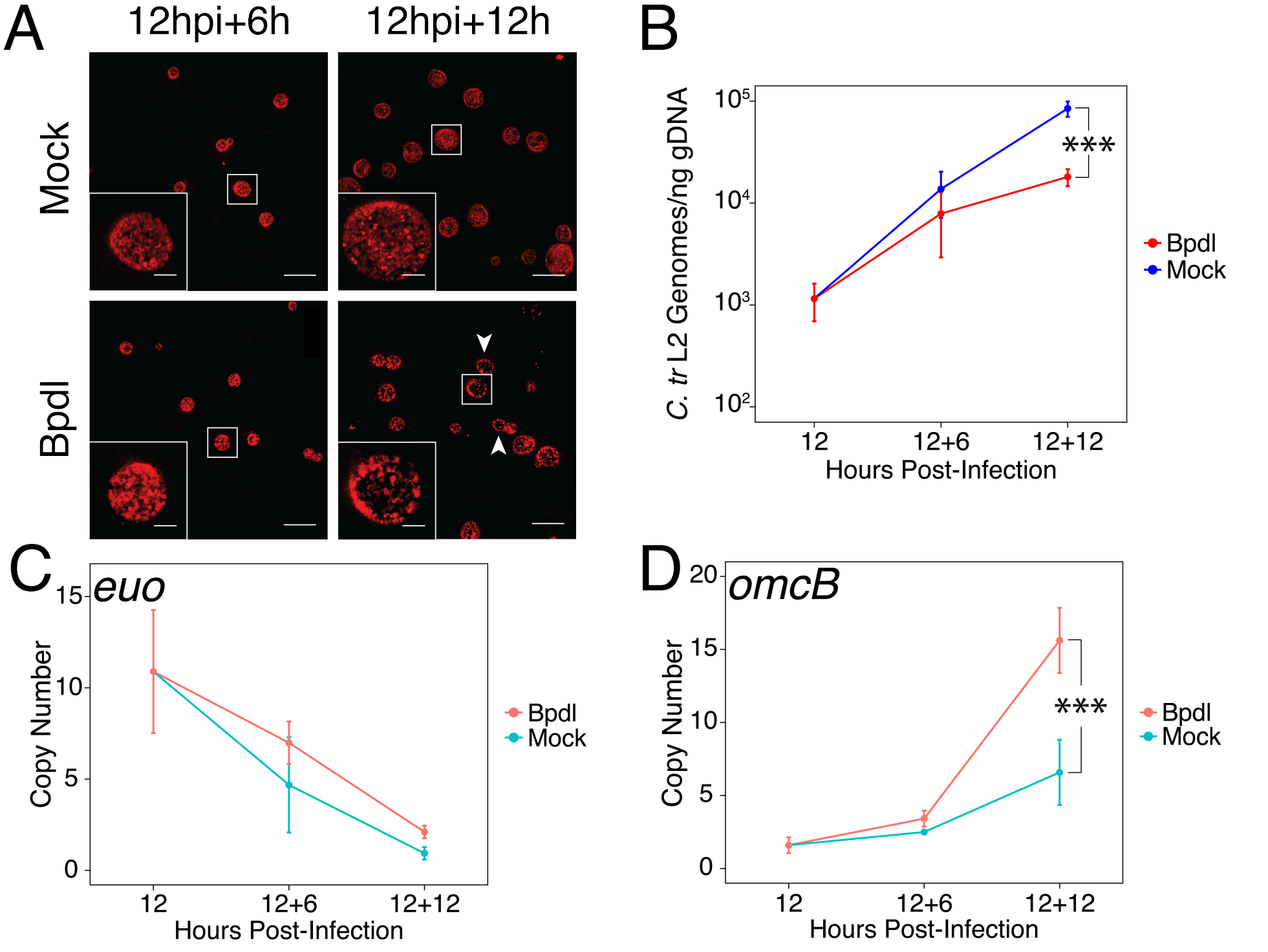
A
12hpi+6h
12hpi+12h
Mock
BpdI
B
C. tr L2 Genomes/ng gDNA
10^5
10^4
10^3
10^2
***
12
12+6
12+12
Hours Post-Infection
BpdI
Mock
C
euo
Copy Number
15
10
5
0
12
12+6
12+12
Hours Post-Infection
BpdI
Mock
D
omcB
Copy Number
20
15
10
5
0
***
12
12+6
12+12
Hours Post-Infection
BpdI
Mock

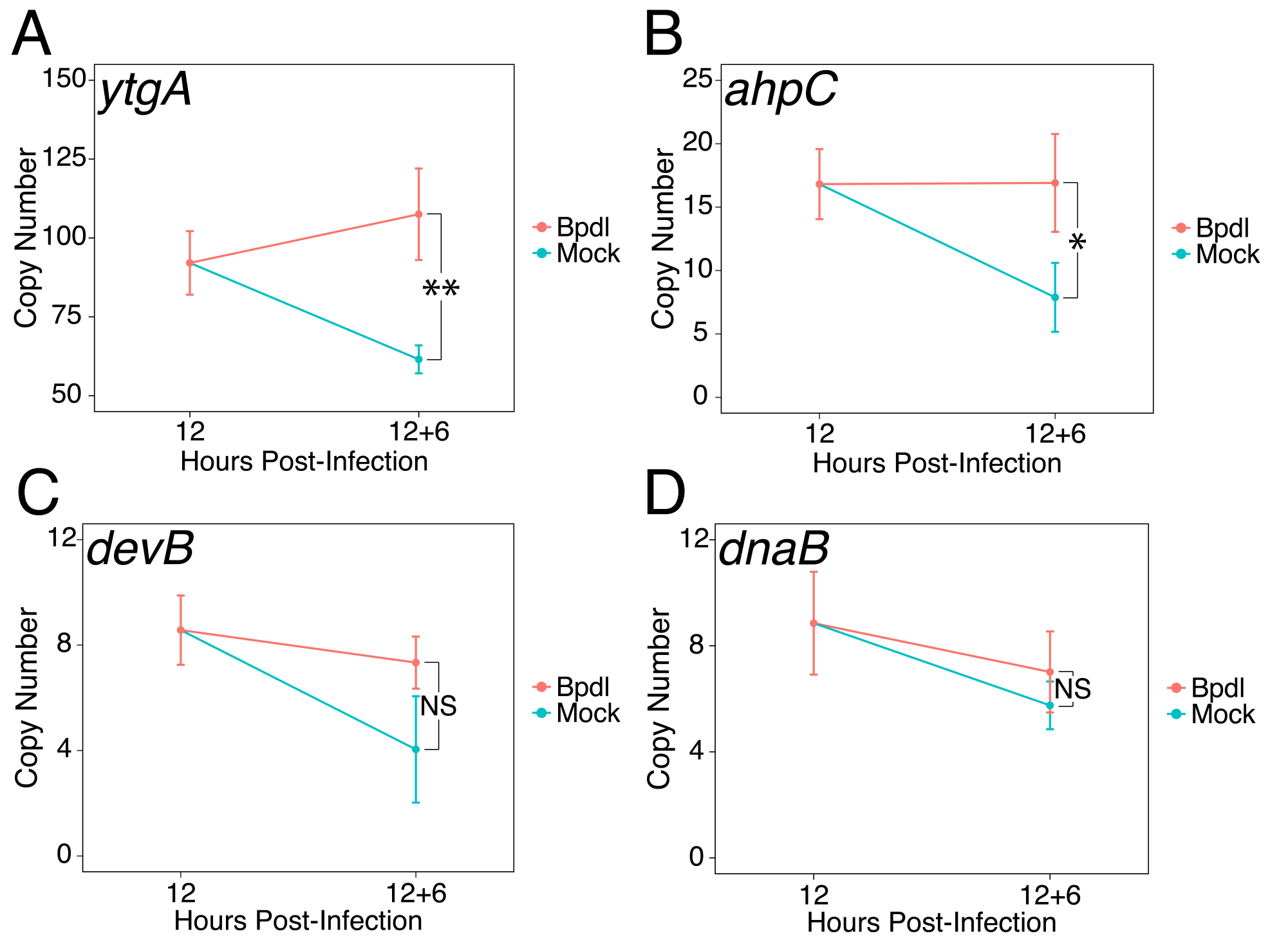
A
ytgA
150
125
100
75
50
Copy Number
**
12
12+6
Hours Post-Infection
BpdI
Mock
B
ahpC
25
20
15
10
5
0
Copy Number
*
12
12+6
Hours Post-Infection
BpdI
Mock
C
devB
12
8
4
0
Copy Number
NS
12
12+6
Hours Post-Infection
BpdI
Mock
D
dnaB
12
8
4
0
Copy Number
NS
12
12+6
Hours Post-Infection
BpdI
Mock

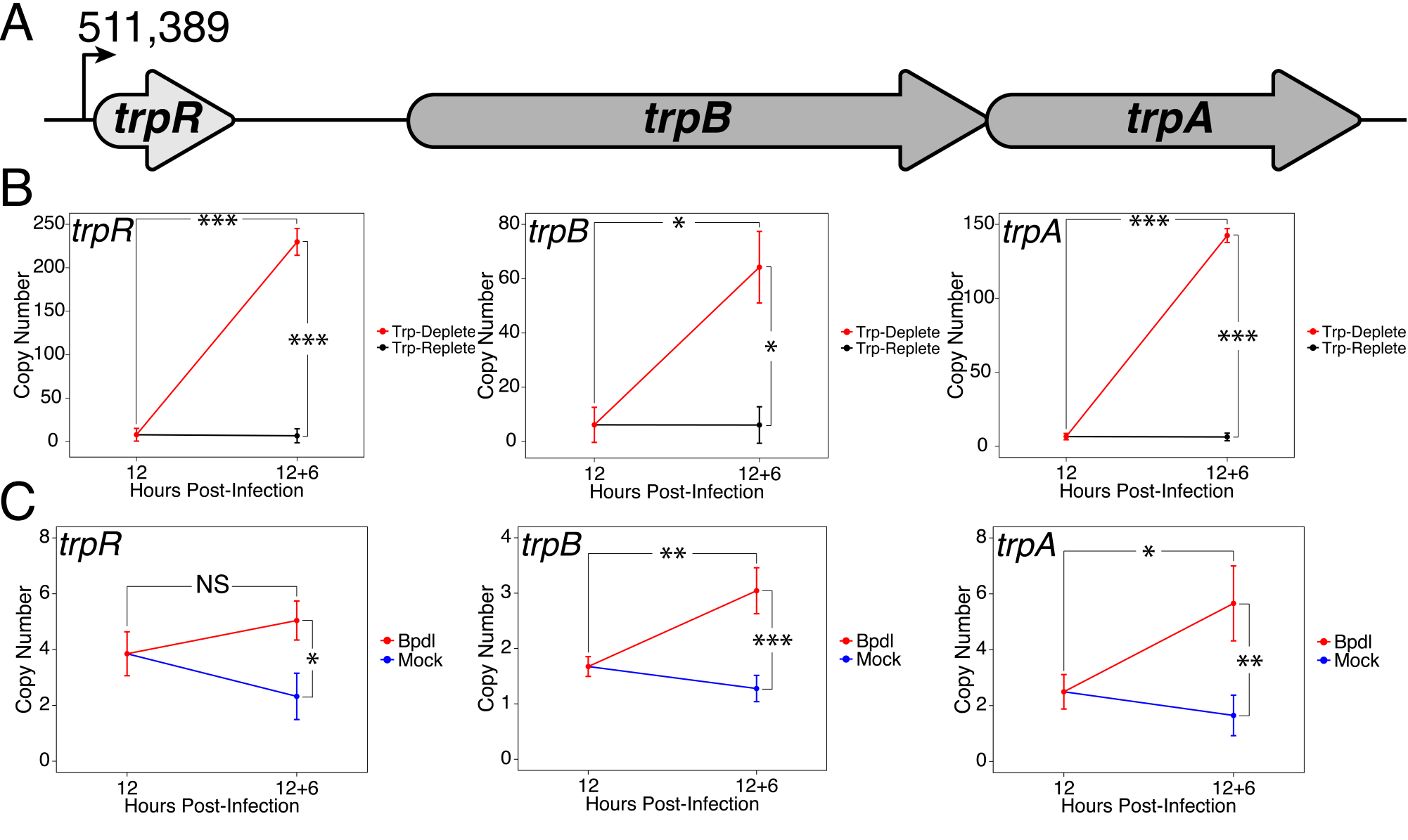
A
511,389
trpR
trpB
trpA
B
trpR
***
***
Copy Number
250
200
150
100
50
0
12
12+6
Hours Post-Infection
Trp-Deplete
Trp-Replete
trpB
*
*
Copy Number
80
60
40
20
0
12
12+6
Hours Post-Infection
Trp-Deplete
Trp-Replete
trpA
***
***
Copy Number
150
100
50
0
12
12+6
Hours Post-Infection
Trp-Deplete
Trp-Replete
C
trpR
NS
*
Copy Number
8
6
4
2
0
12
12+6
Hours Post-Infection
BpdI
Mock
trpB
**
***
Copy Number
4
3
2
1
0
12
12+6
Hours Post-Infection
BpdI
Mock
trpA
*
**
Copy Number
8
6
4
2
0
12
12+6
Hours Post-Infection
BpdI
Mock

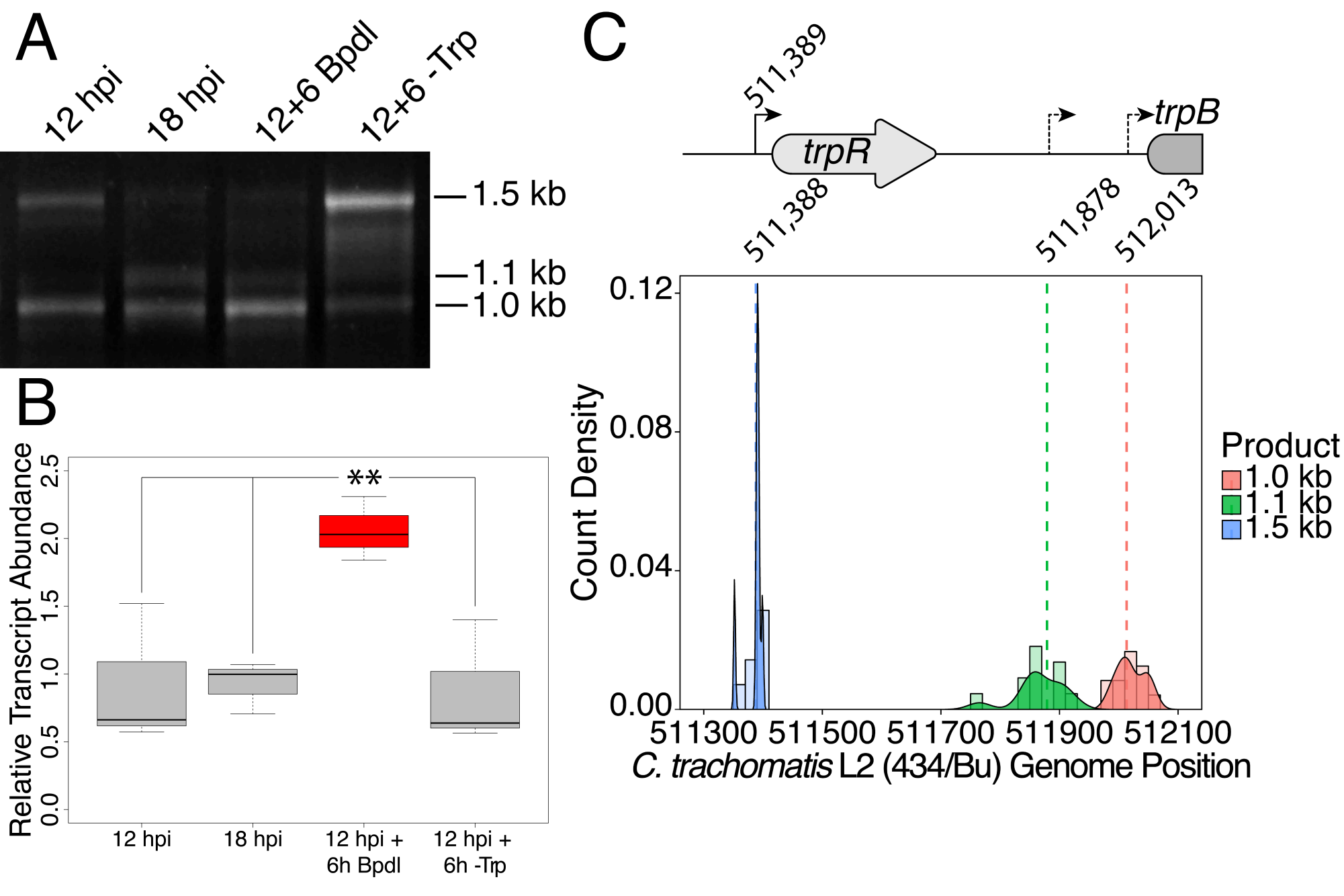
A
12 hpi
18 hpi
12+6 BpdI
12+6 -Trp
1.5 kb
1.1 kb
1.0 kb
B
Relative Transcript Abundance
0.0
0.5
1.0
1.5
2.0
2.5
**
12 hpi
18 hpi
12 hpi + 6h BpdI
12 hpi + 6h -Trp
C
511,389
trpR
trpB
511,388
511,878
512,013
Count Density
0.00
0.04
0.08
0.12
511300 511500 511700 511900 512100
C. trachomatis L2 (434/Bu) Genome Position
Product
1.0 kb
1.1 kb
1.5 kb

A

	Local Pairwise Alignment	Identity
YtgR Operator *trpRBA* IGR	2 CTCTTCGAGATGA 14 123 CTTTTCAAGCTGA 135	76.9%

	Global Pairwise Alignment	Identity
YtgR Operator Palindrome	1 -----TCTCTTCGAGATGAGAAA 18 1 AATCAGCTTTTCAAGCTGAT T-- 21	43.5%

Palindrome	5’ AATCAGCTTTTCAAGCTGATT	3’
Mutated Palindrome	CGGCGGCGCGGCAAGCTGATT	

B

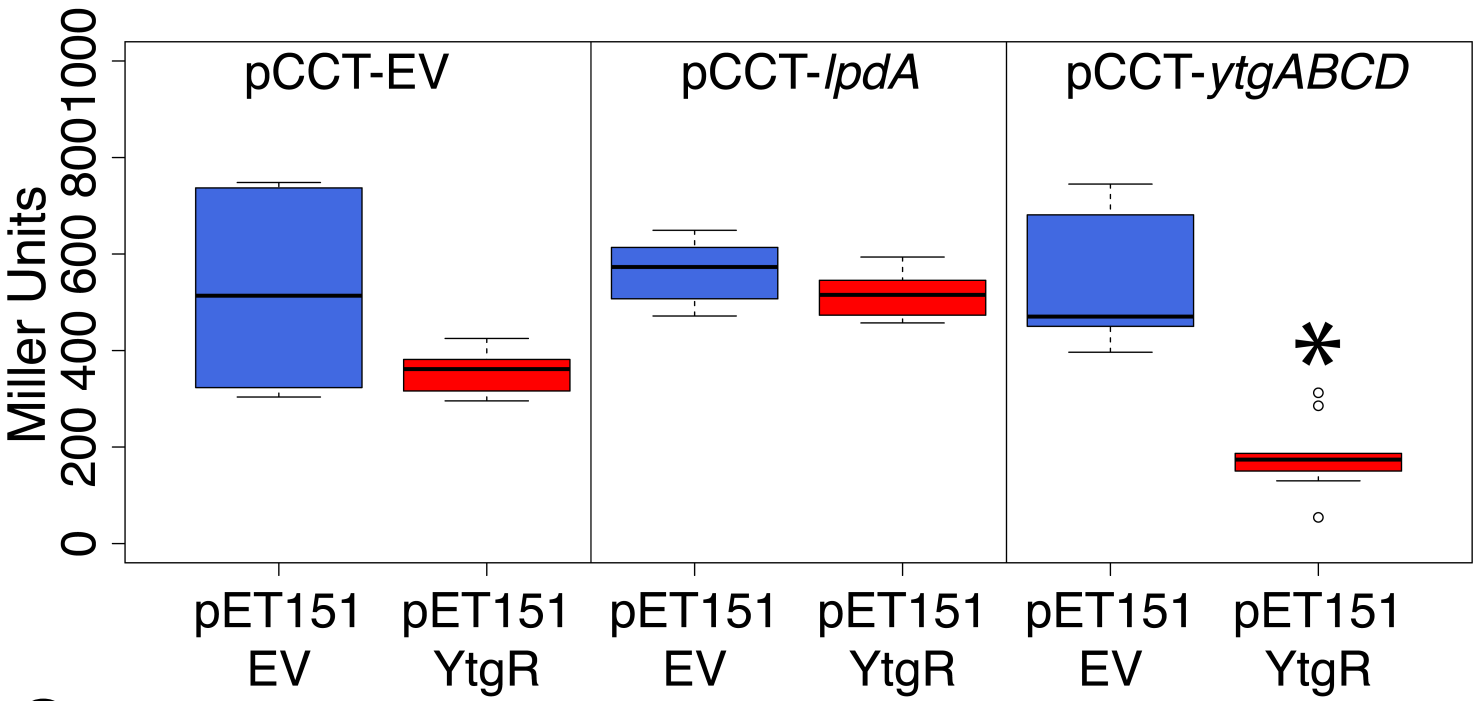

C

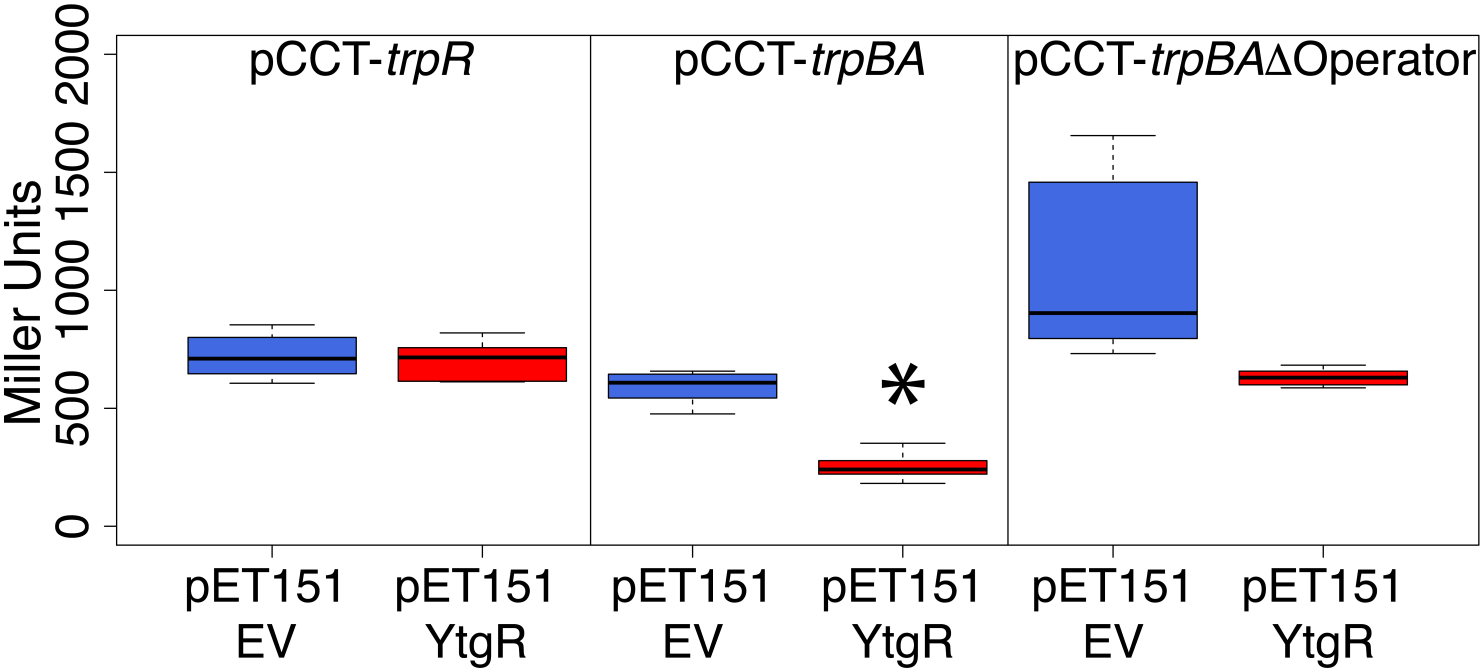

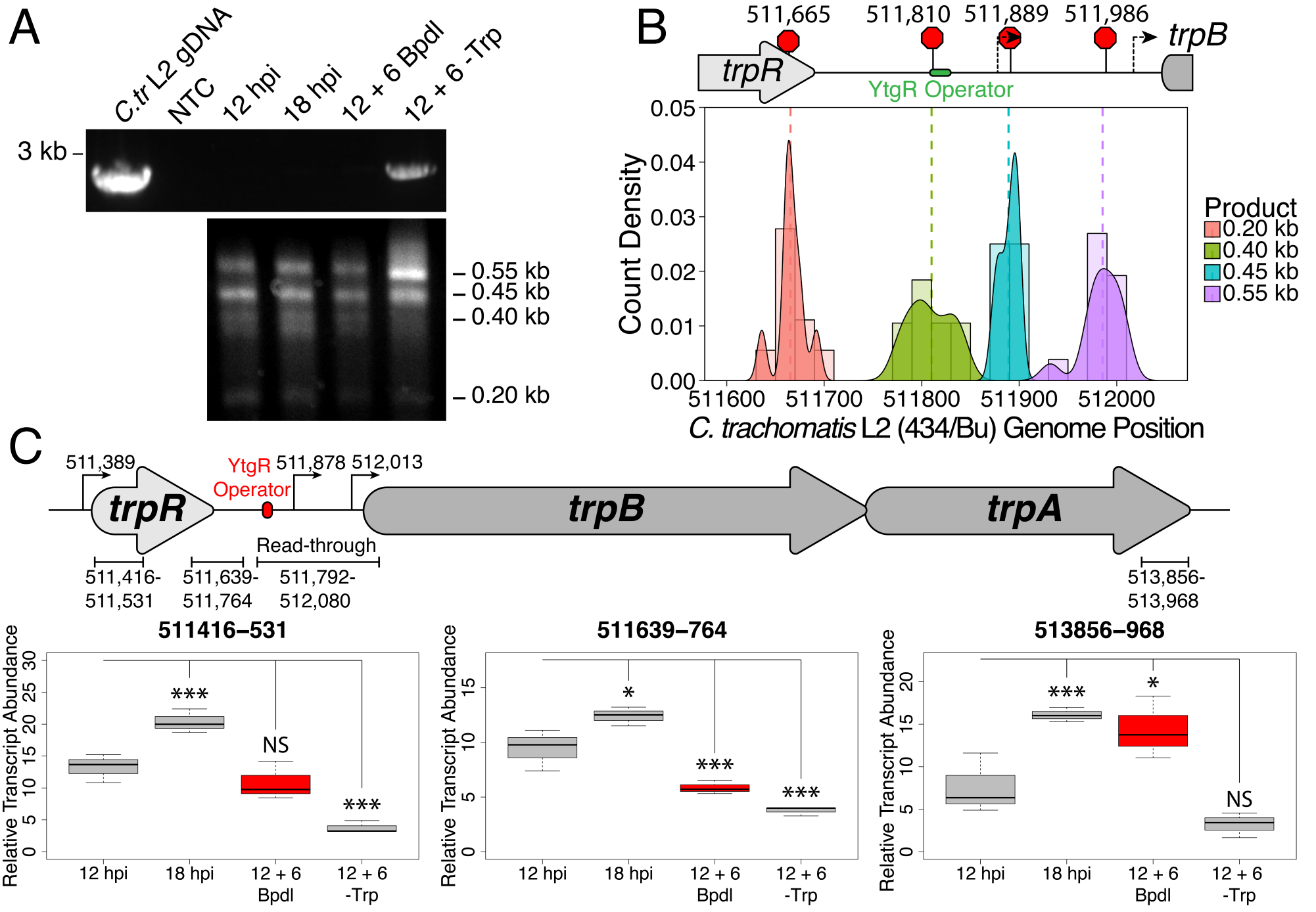
A
C.tr L2 gDNA
NTC
12 hpi
18 hpi
12 + 6 BpdI
12 + 6 -Trp
3 kb
0.55 kb
0.45 kb
0.40 kb
0.20 kb
B
511,665
511,810
511,889
511,986
trpB
trpR
YtgR Operator
Count Density
0.05
0.04
0.03
0.02
0.01
0.00
511600
511700
511800
511900
512000
C. trachomatis L2 (434/Bu) Genome Position
Product
0.20 kb
0.40 kb
0.45 kb
0.55 kb
C
511,389
YtgR Operator
511,878
512,013
trpR
trpB
trpA
Read-through
511,416-
511,531
511,639-
511,764
511,792-
512,080
513,856-
513,968
511416–531
511639–764
513856–968
Relative Transcript Abundance
12 hpi
18 hpi
12 + 6 BpdI
12 + 6 -Trp
***
NS
*